# Strong electro-osmotic flows about dielectric surfaces of zero surface charge

Ory Schnitzer and Ehud Yariv
*Department of Mathematics, Technion–Israel Institute of Technology, Haifa 32000, Israel*
(Received 31 December 2013; published 4 April 2014)

We analyze electro-osmotic flow about a dielectric solid of zero surface charge, using the prototypic configurations of a spherical particle and an infinite circular cylinder. We assume that the ratio $\delta$ of Debye width to particle size is asymptotically small, and consider the flow engendered by the application of a uniform electric field; the control parameter is $E$—the voltage drop on the particle (normalized by the thermal scale) associated with this field. For moderate fields, $E = O(1)$, the induced $\zeta$ potential scales as the product of the applied-field magnitude and the Debye width; being small compared with the thermal voltage, its resolution requires addressing one higher asymptotic order than that resolved in the comparable analysis of electrophoresis of charged particles. For strong fields, $E = O(\delta^{-1})$, the $\zeta$ potential becomes comparable to the thermal voltage, depending nonlinearly on $\delta$ and $E$. We obtain a uniform approximation for the $\zeta$-potential distribution, valid for both moderate and strong fields; it holds even under intense fields, $E \gg \delta^{-1}$, where it scales as $\log|E|$. The induced-flow magnitude therefore undergoes a transition from an $E^2$ dependence at moderate fields to an essentially linear variation with $|E|$ at intense fields. Remarkably, surface conduction is negligible as long as $E \ll \delta^{-2}$: the $\zeta$ potential, albeit induced, remains mild even under intense fields. Thus, unlike the related problem of induced-charge flow about a perfect conductor, the theoretical velocity predictions in the present problem may actually be experimentally realized.

DOI: 10.1103/PhysRevE.89.043005 PACS number(s): 47.57.jd, 47.61.−k, 66.10.Ed, 47.15.G−

## I. INTRODUCTION

### A. Counterintuitive problem

Consider a chemically inert dielectric particle suspended in an electrolyte solution. By varying the solution pH one can reach the isoelectric point, where the electrical charge density on the particle boundary is zero. No double layer is formed, and the cations and anions are uniformly distributed. When consulting with standard textbooks in the field one may get the impression that no electrokinetic flow would be generated when an external electric field is applied. The calculation of the electric-field distribution will then appear to belong to the realm of electrostatics. Such an "electrostatic" distribution, however, is incompatible with the ohmic nature of a uniform electrolyte solution, where electric fields are accompanied by electric currents (through cations moving with the field and anions moving against it): for any finite ratio $\gamma$ of the solid-to-liquid permittivity values, the electric field at the surface would possess a normal component, which would paradoxically deliver electric current into or out of an inert solid.

The present scenario thus falls into the category of induced-charge electro-osmosis [1,2]. An induced diffuse-charge ("Debye") layer must develop about the surface, modifying the streamline pattern predicted by the "purely electrostatic" calculation. The action of the electric field on the charged liquid within this layer results in Coulomb body forces, which, in turn, animate electrokinetic flow. This is most evident in the limit of thin Debye layers, where the ratio $\delta$ of Debye width to particle size is asymptotically small. In steady state, the field lines outside the Debye layer must be approximately tangential to the surface. This situation clearly resembles induced-charge flow about a perfectly conducting (metal) particle, discussed in detail in Ref. [2] in the limit of small $\delta$. There is, however, a crucial difference: in the case of a perfect conductor, the surface acquires a (nonuniform) charge distribution opposing that in the diffuse layer (microscopically, this distribution is formed through rearrangement of electrons within the metal); a double layer is accordingly formed, albeit in an induced fashion. No such surface charge appears on the boundary of the dielectric particle [3]. Thus, in the latter case there is no "net" macroscopic electroneutrality in a slab-shaped control volume spanning the diffuse layer and the solid surface [4]. Common intuition, based upon small deviations from equilibrium, is here misleading.

The resemblance also breaks down when considering the mathematical modeling in the limit of thin Debye layers. In the scheme presented by Squires and Bazant [2] for the case of perfect conductors, the electric potential is first calculated in the electroneutral "bulk" fluid, outside the thin Debye layer. The $\zeta$ potential, namely the voltage across the Debye layer, is then found by subtracting the resulting electric potential distribution, evaluated at the bulk boundary, from the uniform value of the electric potential in the conducting solid. The resulting distribution of induced $\zeta$ potential scales as the product of the applied-field magnitude and the linear dimension of the particle. This scheme is inapplicable for a dielectric solid in which the electric potential is nonuniform, and, in any event, cannot be determined in that fashion. An example of an erroneous attempt to adopt the procedure of Squires and Bazant to the case of an uncharged dielectric solid can be found in a recent paper by Zhang and Li [5]: for moderate ratios of $\gamma$ their expression for the $\zeta$ potential [see their Eq. (6)] is absurdly of the same scaling as that found in Ref. [2] for a perfect conductor.

### B. Present state of knowledge

The erroneous expression obtained by Zhang and Li [5] is only a symptom of the existing confusion associated with the effect of dielectric-solid polarization on electrokinetic phenomena. Before heading to analyze the specific problem of

 

induced-charge flow about an uncharged dielectric solid, it is expedient to review the relevant literature discussing various effects of solid polarization in the limit of thin Debye layers.

Solid polarization is traditionally neglected in analyses of electrokinetic phenomena [6]. In the past decade, however, it became evident that solid polarization plays a key role in electrokinetic flows about sharp corners [7,8] and microchannel junctions [9], as well as in nonconventional configurations involving dielectric stripes over electrodes [10]. The effect of dielectric-solid polarization was reviewed by Squires and Bazant [2] in their unified treatment of induced-charge flows. While their general discussion regards metals and dielectrics on the same par ("polarizable" materials), their analysis tends to focus on the former, with configurations involving dielectric surfaces presented in less detail. One such configuration is a dielectric cylinder coated by another dielectric material, for which the authors provide the final expression for the induced $\zeta$ potential. Of special interest is their result (6.13) appropriate to the limit of vanishing coating thickness (i.e., a single dielectric material). For moderate values of the ratio $\gamma$ of solid-to-liquid dielectric constants, their expression reveals that the $\zeta$ potential scales as the product of the applied-field magnitude and the Debye thickness, in marked contrast with the scaling corresponding to a perfect conductor. This appears to be the first analysis of electro-osmotic flows about an uncharged dielectric surface.

The technical procedure for dealing with solid polarization was explicitly detailed by Yossifon, Frankel, and Miloh [11]. Assuming low $\zeta$ potentials (the Debye-Hückel limit), the authors showed that the electric potential within the solid satisfies a Robin-type boundary condition, governed by the parameter

$$\alpha = \delta\gamma \tag{1.1}$$

(which has already appeared in Ref. [2]); this work was later generalized to allow for nonsmall $\zeta$ potentials [12]. The results in Ref. [11] indicate that for dielectric materials which are realistically encountered in electrokinetic applications, where $\gamma$ is at most moderate [13], the induced $\zeta$ potential is proportional to the Debye width, in agreement with the predictions of Squires and Bazant [2]. (This result alone clearly indicates that the calculation of Zhang and Li [5] is erroneous.)

It is important to emphasize, however, that the analysis in Refs. [2,11,12] makes use of the standard bulk description appropriate to the thin-double-layer limit, which neglects terms which are $O(\delta)$ small. While this is legitimate if one implicitly assumes that $\alpha$ is $O(1)$, it is not *a priori* self-consistent for realistic dielectric materials, where (1.1) implies that $\alpha$ is at most $O(\delta)$, as is then the induced $\zeta$ potential. More importantly, it is clear that the approach in these papers is unsuitable for the case where the applied field is strong: this limit, which is actually prevailing in many practical applications, has never been addressed in the context of induced-charge flows.

### C. Plan of operation

In what follows we systematically address the problem of electro-osmotic flow about an uncharged dielectric particle for both moderate and strong fields (the distinction will be made clear later on). For brevity we elect to illuminate the electrokinetic transport in the simplest context which is nonetheless representative. The configuration we choose consists of a spherical particle exposed to a uniform and constant electric field. Following the analysis pertaining to this geometry, we briefly present the comparable key results for the two-dimensional flow about an infinite circular cylinder. In analyzing the problem, we employ inner-outer asymptotic expansions in a fashion resembling our earlier analysis of more "conventional" electrokinetic phenomena involving charged dielectric solids [14]. It is important to emphasize, however, that, owing to the absence of an electroneutral double-layer structure (either fixed or induced) in the present problem, the present analysis is necessarily different.

Prior to carrying out the analysis, several remarks are in place concerning the assumption of an uncharged surface. This assumption may raise some concerns since the process of surface-charge formation is a statistical one, which inevitably results in charge fluctuations: even when tuning the conditions in an electrolyte (e.g., the pH) in such a way that the surface charge vanishes, it does so only on average [15]. Nonetheless, the idealization of an uncharged surface is instrumental in focusing upon the unique features of electrokinetic flows animated by solid polarization. Moreover, the results obtained for electro-osmosis under intense electric fields, and especially the unique velocity scaling [see, e.g., Eq. (5.11)], imply that the solid-polarization mechanism would dominate "conventional" electro-osmotic flow provided the "equilibrium" $\zeta$ potential is small compared with the thermal voltage. The electrokinetic analysis under the assumption of a zero surface charge may accordingly provide a leading-order description for the flow about a *weakly* charged particle.

## II. PROBLEM FORMULATION

A chemically inert solid sphere (radius $a^*$) is suspended in a symmetric (valencies $\pm\mathcal{Z}$) electrolyte solution, whose two ionic species possess the diffusivities $D^{*\pm}$ (dimensional quantities being hereafter decorated by an asterisk). This solution is treated as a dielectric Newtonian liquid (permittivity $\epsilon^*$; viscosity $\mu^*$). The solid particle is dielectric, with permittivity $\gamma\epsilon^*$.

The particle boundary is assumed uncharged. Thus, in the absence of an applied field, both ionic species possess uniform concentrations; the concentrations are identical, say of value $c^*$, and the electric potential is uniform throughout. Our interest lies in the steady-state flow resulting from the application of a uniform and constant electric field of magnitude $E^*$. In view of the inherent fore-aft symmetry in the problem, it is legitimate to consider a stationary sphere.

In describing the governing equations we employ a dimensionless formulation, normalizing length variables by $a^*$, the two ionic concentrations by $c^*$, and the electric potentials by the thermal scale ($\approx$26 mv for univalent solutions at room temperature),

$$\varphi^* = \frac{k^*T^*}{\mathcal{Z}e^*}, \tag{2.1}$$

in which $k^*T^*$ is the Boltzmann temperature and $e^*$ the elementary charge. The pressure is normalized by the Maxwell

scale $\epsilon^*\varphi^{*2}/a^{*2}$ and the velocities by

$$\frac{\epsilon^*\varphi^{*2}}{a^*\mu^*}. \tag{2.2}$$

### A. Liquid transport

The electrokinetic transport within the fluid is described in terms of the two ionic concentrations $c^\pm$, the electric potential $\varphi$, the velocity field $\mathbf{u}$, and the pressure $p$. These variables satisfy the following differential equations.

(1) Nernst-Planck ionic conservation:

$$\nabla\cdot\mathbf{j}^\pm + m^\pm\mathbf{u}\cdot\nabla c^\pm = 0. \tag{2.3}$$

Here, the molecular ionic fluxes $\mathbf{j}^\pm$ (respectively normalized by $D^{*\pm}c^*/a^*$) are provided by the constitutive expressions

$$\mathbf{j}^\pm = -\nabla c^\pm \mp c^\pm\nabla\varphi \tag{2.4}$$

describing transport due to the combined action of diffusion and electromigration. The dimensionless groups

$$m^\pm = \frac{\epsilon^*\varphi^{*2}}{\mu^*D^{*\pm}}, \tag{2.5}$$

multiplying the advection terms, represent the ionic drag coefficients; these groups are independent of both $a^*$ and $c^*$; for typical diffusivities ($\approx 10^{-9}\mathrm{m}^2\mathrm{s}^{-1}$) in univalent aqueous solutions ($\mu^* \approx 10^{-3}\mathrm{kgm}^{-1}s^{-1}$), they are $\lesssim 0.5$ [16].

(2) Poisson:

$$-2\delta^2\nabla^2\varphi = c^+ - c^-. \tag{2.6}$$

Here,

$$\delta = \frac{\lambda^*}{a^*} \tag{2.7}$$

is the ratio of the Debye width

$$\lambda^* = \sqrt{\frac{\epsilon^*\varphi^*}{2\mathcal{Z}e^*c^*}} \tag{2.8}$$

to particle size.

(3) Mass conservation:

$$\nabla\cdot\mathbf{u} = 0. \tag{2.9}$$

(4) Inhomogeneous Stokes equation:

$$\nabla p = \nabla^2\mathbf{u} + \nabla^2\varphi\nabla\varphi, \tag{2.10}$$

governing the inertialess motion of the fluid, subject to Coulomb body forces.

### B. Boundary conditions

The boundary conditions are conveniently prescribed using spherical coordinates $(r,\theta,\varpi)$ with $r$ measured from the particle center and $\theta = 0$ in the applied-field direction. Because of axial symmetry, the velocity field adopts the form $\mathbf{u} = \hat{\mathbf{e}}_r u + \hat{\mathbf{e}}_\theta v$. All scalar variables, as well as $u$ and $v$, are independent of the azimuthal angle $\varpi$.

On the particle boundary, $r = 1$, we have the following.

(1) No flux of ions:

$$\hat{\mathbf{e}}_r\cdot\mathbf{j}_\pm = 0, \tag{2.11}$$

representing the inability of the solution ions to discharge on the chemically inert solid surface.

(2) Electric-potential continuity:

$$\varphi = \grave{\varphi}, \tag{2.12}$$

in which $\grave{\varphi}$ is the electric potential within the dielectric solid.

(3) Electric-displacement continuity:

$$\frac{\partial\varphi}{\partial r} = \gamma\frac{\partial\grave{\varphi}}{\partial r}, \tag{2.13}$$

representing Gauss's boundary condition in the absence of surface charge.

(4) Impermeability to flow:

$$u = 0. \tag{2.14}$$

(5) No slip:

$$v = 0. \tag{2.15}$$

Additional conditions apply at large distances from the particle, as $r \to \infty$, where the ionic concentrations approach their equilibrium value,

$$c^\pm \to 1, \tag{2.16}$$

the flow attenuates,

$$\mathbf{u} \to \mathbf{0}, \tag{2.17}$$

and the electric field becomes uniform,

$$\varphi \sim -Er\cos\theta. \tag{2.18}$$

Here,

$$E = \frac{a^*E^*}{\varphi^*} \tag{2.19}$$

is the dimensionless magnitude of the applied field.

### C. Within the solid

Conditions (2.12) and (2.13) couple the transport within the liquid to the electric potential $\grave{\varphi}$ within the solid; since no charge is present there, Poisson's equation yields

$$\nabla^2\grave{\varphi} = 0. \tag{2.20}$$

### D. Alternative formulation

As an alternative to the use of $c^\pm$ we can employ the average ("salt") concentration (normalized by $c^*$) and volumetric charge density (normalized by $2\mathcal{Z}e^*c^*$),

$$c = \tfrac{1}{2}(c^+ + c^-), \quad q = \tfrac{1}{2}(c^+ - c^-). \tag{2.21}$$

Defining

$$\mathbf{j} = \tfrac{1}{2}(\mathbf{j}^+ + \mathbf{j}^-), \quad \mathbf{i} = \tfrac{1}{2}(\mathbf{j}^+ - \mathbf{j}^-), \tag{2.22}$$

we find, using (2.4),

$$\mathbf{j} = -\nabla c - q\nabla\varphi, \quad \mathbf{i} = -\nabla q - c\nabla\varphi. \tag{2.23}$$

Mutual addition and subtraction of the Nernst-Planck equations (2.3) respectively yield the salt and charge balances,

$$\nabla\cdot\mathbf{j}+\frac{m^+ + m^-}{2}\mathbf{u}\cdot\nabla c+\frac{m^+ - m^-}{2}\mathbf{u}\cdot\nabla q=0, \tag{2.24}$$

$$\nabla\cdot\mathbf{i}+\frac{m^+ - m^-}{2}\mathbf{u}\cdot\nabla c+\frac{m^+ + m^-}{2}\mathbf{u}\cdot\nabla q=0. \tag{2.25}$$

In addition, Poisson's equation (2.6) becomes

$$-2\delta^2\nabla^2\varphi = q. \tag{2.26}$$

Lastly, when expressed in terms of the reduced variables, the no-flux conditions (2.11) become

$$\hat{\mathbf{e}}_r\cdot\mathbf{j}=0,\quad \hat{\mathbf{e}}_r\cdot\mathbf{i}=0, \tag{2.27}$$

while the far-field conditions (2.16) read

$$c\to 1,\quad q\to 0. \tag{2.28}$$

## III. THIN DEBYE LAYER

We consider the limit of thin Debye width, $\delta\ll 1$. In what follows, we assume that all other parameters are $O(1)$. We therefore restrict the investigation here to moderate fields,

$$E = O(1). \tag{3.1}$$

The comparable analysis for strong fields is performed in Sec. IV.

We employ the generic expansion

$$f(r,\theta;\delta) = f_0(r,\theta)+\delta f_1(r,\theta)+\cdots. \tag{3.2}$$

With $\varphi$ being $O(1)$, Poisson's equation (2.26) readily yields electroneutrality at both $O(1)$ and $O(\delta)$,

$$q_0\equiv 0,\quad q_1\equiv 0, \tag{3.3}$$

implying that

$$\mathbf{j}_0=-\nabla c_0,\quad \mathbf{i}_0=-c_0\nabla\varphi_0. \tag{3.4}$$

At $O(1)$, the salt and charge balances (2.24) and (2.25), respectively, read

$$\nabla^2 c_0=\frac{m^+ + m^-}{2}\mathbf{u}_0\cdot\nabla c_0, \tag{3.5}$$

$$\nabla\cdot(c_0\nabla\varphi_0)=\frac{m^+ - m^-}{2}\mathbf{u}_0\cdot\nabla c_0. \tag{3.6}$$

The no-flux condition (2.27) in conjunction with (3.4) yield the homogeneous boundary conditions

$$\frac{\partial c_0}{\partial r}=0,\quad \frac{\partial\varphi_0}{\partial r}=0. \tag{3.7}$$

In view of the homogenous differential equation (3.5) and far-field condition governing $c_0-1$, we obtain the uniform concentration:

$$c_0\equiv 1. \tag{3.8}$$

It then follows from (3.6) that $\varphi_0$ is harmonic

$$\nabla^2\varphi_0=0. \tag{3.9}$$

Since it also satisfies the far-field condition,

$$\varphi_0\sim -Er\cos\theta, \tag{3.10}$$

all that remains is to apply the appropriate boundary condition at $r=1$. The second of (3.7) then yields

$$\varphi_0=-E\left(r+\frac{1}{2r^2}\right)\cos\theta. \tag{3.11}$$

### A. Incompatibility with Gauss's law?

Rather than applying the second of (3.7), one could in principle determine $\varphi_0$ using the electrostatic boundary conditions,

$$\varphi_0=\hat{\varphi}_0,\quad \frac{\partial\varphi_0}{\partial r}=\gamma\frac{\partial\hat{\varphi}_0}{\partial r}. \tag{3.12}$$

The solution for Laplace's equation governing $\varphi_0$ and $\hat{\varphi}_0$ satisfying these conditions together with (3.10) is well known:

$$\varphi_0=-E\left(r-\frac{\gamma-1}{\gamma+2}r^{-2}\right)\cos\theta,\quad \hat{\varphi}_0=-\frac{3Er\cos\theta}{\gamma+2}. \tag{3.13}$$

This is different from (3.11).

### B. Singular limit

The apparent inconsistency reflects the familiar singular nature of the limit $\delta\ll 1$, associated with the multiplication of the small expansion parameter by the highest derivative in Poisson's equation (2.26). It implies that the preceding expansions are nonuniform: a boundary ("Debye") layer of $O(\delta)$ width develops about the interface $r=1$. Note that in the present problem a diffuse-charge layer forms despite the absence of surface charge.

The generic expansion described by (3.2) thus applies to the outer region, outside the boundary layer; the boundary conditions on the interface apply to the inner Debye-scale fields. The error in (3.12) has to do with the application of boundary conditions to the outer fields. The correct approach is to separately analyze the inner and outer regions, and then use asymptotic matching to derive effective boundary conditions governing the electrokinetic transport in the outer domain. Use of such inner-outer asymptotic expansions is widespread in electrokinetic analyses [14,17]. We now apply this approach in the delicate case of an uncharged dielectric surface.

To emphasize the distinction between the two domains, we use $\bar{r}$ for the radial coordinate in the outer region. Thus $\bar{r}=1$ represents the effective boundary, rather than the literal interface $r=1$, where the boundary conditions are specified. The $O(\delta)$-wide Debye layer is resolved using the stretched radial coordinate

$$Z=\frac{r-1}{\delta}, \tag{3.14}$$

whereby the boundary conditions apply at $Z=0$. The generic expansion in the inner region, replacing (3.2), is

$$f(r,\theta;\delta)=F_0(Z,\theta)+\delta F_1(Z,\theta)+\cdots. \tag{3.15}$$

Specifically, the radial components of the ionic fluxes are expanded as

$$\hat{\mathbf{e}}_r\cdot\mathbf{j}^{\pm}=J_0^{\pm}(Z,\theta)+\delta J_1^{\pm}(Z,\theta)+\cdots. \tag{3.16}$$

The previous nonuniformity can readily be clarified. In the inner region, the Nernst-Planck equations (2.3) at $O(\delta^{-1})$ read $\partial J_0^{\pm}/\partial Z = 0$; the no-flux conditions (2.11) thus give

$$J_0^{\pm} \equiv 0. \tag{3.17}$$

Asymptotic matching with the outer region then provides the effective conditions

$$\hat{\mathbf{e}}_r \cdot \mathbf{j}_0 = 0, \quad \hat{\mathbf{e}}_r \cdot \mathbf{i}_0 = 0 \quad \text{at} \quad \bar{r} = 1. \tag{3.18}$$

Using (3.4) it then follows that conditions (3.7) still apply, but are now understood to hold at $\bar{r} = 1$ (with the partial differentiation being carried with respect to $\bar{r}$). It follows that (3.8)–(3.11) remain valid (with $\bar{r}$ replacing $r$ throughout).

### C. Absence of $\zeta$ potential and electro-osmosis at $O(1)$

Following standard Debye-scale analyses [14], we start by noting the absence of $O(\delta^{-1})$ radial fluxes. Using (2.4), this implies

$$-\frac{\partial C_0^{\pm}}{\partial Z} \mp C_0^{\pm} \frac{\partial \Phi_0}{\partial Z} = 0. \tag{3.19}$$

Integration of (3.19) in conjunction with asymptotic matching provides the Boltzmann distributions

$$C_0^{\pm} = e^{\mp \Psi}, \tag{3.20}$$

wherein

$$\Psi = \Phi_0 - \varphi_0 \tag{3.21}$$

is the "excess" Debye-layer potential, relative to the bulk potential at $\bar{r} = 1$. (In what follows, outer variables appearing in the Debye-scale analysis are understood to be evaluated at this effective boundary.) Substitution into Poisson's equation (2.26) yields at leading order

$$\frac{\partial^2 \Psi}{\partial Z^2} = \sinh \Psi. \tag{3.22}$$

This equation is subject to large-$Z$ decay together with the leading $O(\delta^{-1})$ balance of Gauss's condition (2.13)

$$\frac{\partial \Psi}{\partial Z} = 0 \quad \text{at} \quad Z = 0. \tag{3.23}$$

In contrast to standard electrokinetic analysis involving charged surfaces [14], here Gauss's law stipulates a *homogeneous* boundary condition. It follows that $\Psi \equiv 0$, whereby $\Phi_0$ is independent of $Z$:

$$\Phi_0(\theta) = \varphi_0. \tag{3.24}$$

The $\zeta$ potential thus vanishes at $O(1)$. In addition, (3.20) yields

$$C_0^{\pm} \equiv 1. \tag{3.25}$$

Thus, unlike standard Debye-scale analyses [14], here we find that the leading-order electrochemical fields simply constitute a trivial extrapolation of the respective outer fields. (As will become evident in the next section, the situation is different in the case of strong fields.)

With $\Phi_0$ independent of $Z$, it follows from the momentum balance in the radial direction that the pressure is only $O(1)$ [as apposed to $O(\delta^{-2})$ as in the case of a charged solid [14]]. Moreover, it readily follows from the no-slip condition together with the leading $O(\delta^{-2})$ balance of the Stokes equation in the $\theta$ direction that $v$ vanishes at $O(1)$. It therefore possesses the expansion [cf. (3.2)]

$$v = \delta V_1(R,\theta) + \cdots. \tag{3.26}$$

The mass-conservation equation (2.9) in conjunction with the impermeability condition (2.14) thus implies that $u$ is $O(\delta^2)$:

$$u = \delta^2 U_2(R,\theta) + \cdots. \tag{3.27}$$

Asymptotic matching then necessitates that the outer velocity is $O(\delta)$,

$$\mathbf{u} = \delta \mathbf{u}_1 + \cdots. \tag{3.28}$$

It is evident that, unlike the case of a charged solid, determination of the leading-order flow requires here going to one higher asymptotic order. Before proceeding to do so we note that, in view of the transverse uniformity of $\Phi_0$, the $O(1)$ balance of (2.12) in conjunction with (3.11) yields the boundary condition

$$\grave{\varphi}_0 = -\tfrac{3}{2} E \cos\theta \quad \text{at} \quad r = 1. \tag{3.29}$$

Since $\grave{\varphi}_0$ is harmonic, we readily find that the electric field within the solid is uniform:

$$\grave{\varphi}_0 = -\tfrac{3}{2} E r \cos\theta. \tag{3.30}$$

### D. Next asymptotic order

We start with the outer region. With the fluid velocity being $O(\delta)$, the $O(\delta)$ balances of (2.24) and (2.25) are unaffected by convection,

$$\boldsymbol{\nabla} \cdot \mathbf{j}_1 = 0, \quad \boldsymbol{\nabla} \cdot \mathbf{i}_1 = 0. \tag{3.31}$$

Using the $O(\delta)$ electroneutrality [see (3.3)], we find

$$\mathbf{j}_1 = -\boldsymbol{\nabla} c_1, \quad \mathbf{i}_1 = -\boldsymbol{\nabla} \varphi_1 - c_1 \boldsymbol{\nabla} \varphi_0. \tag{3.32}$$

Thus (3.31) yield

$$\nabla^2 c_1 = 0, \quad \nabla^2 \varphi_1 = -\boldsymbol{\nabla} \cdot (c_1 \boldsymbol{\nabla} \varphi_0). \tag{3.33}$$

To obtain effective conditions governing $c_1$ and $\varphi_1$ we now consider the ionic transport in the Debye layer. With the inner velocity scaling (3.26) and (3.27), the Nernst-Planck equations (2.3) at $O(1)$ are still unaffected by ionic advection, $\partial J_1^{\pm}/\partial Z = 0$. The no-flux conditions then give

$$J_1^{\pm} \equiv 0, \tag{3.34}$$

whereby asymptotic matching, in conjunction with (3.7) and (3.32), yields the homogeneous effective conditions

$$\frac{\partial c_1}{\partial \bar{r}} = 0, \quad \frac{\partial \varphi_1}{\partial \bar{r}} = 0 \quad \text{at} \quad \bar{r} = 1. \tag{3.35}$$

Since the far-field conditions [see (2.16) and (2.18)],

$$c_1 \to 0, \quad \varphi_1 \to 0, \tag{3.36}$$

are also homogeneous, it follows that both $c_1$ and $\varphi_1$ vanish. The leading-order velocity is therefore governed by the homogeneous Stokes equations,

$$\boldsymbol{\nabla} \cdot \mathbf{u}_1 = 0, \quad \boldsymbol{\nabla} p_1 = \nabla^2 \mathbf{u}_1. \tag{3.37}$$

Consider now the explicit form of (3.17). Making use of (3.24) and (3.25), they read

$$-\frac{\partial C_1^{\pm}}{\partial Z} \mp \frac{\partial \Phi_1}{\partial Z} = 0. \tag{3.38}$$

The solution that matches (3.36) is

$$C_1^{\pm} = \mp \Phi_1. \tag{3.39}$$

Substitution into Poisson's equation (2.26) at $O(\delta)$ yields the differential equation

$$\frac{\partial^2 \Phi_1}{\partial Z^2} = \Phi_1. \tag{3.40}$$

Its solution, which matches the trivial outer-region potential, is

$$\Phi_1 = A(\theta) e^{-Z}. \tag{3.41}$$

The function $A$ is obtained using the $O(1)$ balance of Gauss's boundary condition (2.13), namely,

$$\left.\frac{\partial \Phi_1}{\partial Z}\right|_{Z=0} = \gamma \left.\frac{\partial \dot{\varphi}_0}{\partial r}\right|_{r=1}. \tag{3.42}$$

Upon substitution of (3.30) we obtain

$$A(\theta) = \tfrac{3}{2}\gamma E \cos\theta. \tag{3.43}$$

We can now calculate $V_1$ using the $O(\delta^{-1})$ momentum balance in the $\theta$ direction,

$$0 = \frac{\partial^2 V_1}{\partial Z^2} + \frac{\partial^2 \Phi_1}{\partial Z^2}\frac{d\Phi_0}{d\theta}. \tag{3.44}$$

Two successive integrations, in conjunction with the requirement of asymptotic matching, yield

$$V_1 = v_1 - \Phi_1 \frac{d\Phi_0}{d\theta}. \tag{3.45}$$

Application of the no-slip condition together with (3.11), (3.24), (3.41), and (3.43) eventually provides the effective slip condition

$$v_1 = \tfrac{9}{4}\gamma E^2 \sin\theta \cos\theta. \tag{3.46}$$

This is supplemented by the effective impermeability condition

$$u_1 = 0, \tag{3.47}$$

which readily follows from matching with the $O(\delta^2)$ radial velocity in the Debye layer.

Equations (3.46) and (3.47), together with the Stokes equations (3.37) and the requirement of far-field decay, uniquely determine $\mathbf{u}_1$. The solution of this equation set is of course well known, since (3.46) possess the same structure as the slip condition on a perfectly conducting sphere [2]. Note that one cannot get the former from the latter by simply applying the limit $\gamma \to \infty$.

## IV. STRONG ELECTRIC FIELDS

The preceding analysis suggests a qualitative difference at strong electric fields, scaling as $\delta^{-1}$, where solid polarization is expected to enter the $O(\delta^{-1})$ balance of Gauss's boundary condition, giving rise to an $O(1)$ $\zeta$ potential. We therefore consider here separately the case where $E$ is of order $\delta^{-1}$. This is expressed by writing

$$E = \delta^{-1}\tilde{E} \tag{4.1}$$

and considering $\tilde{E}$ as an $O(1)$ parameter.

### A. Outer analysis

Clearly, the generic expansion (3.2) is not general enough for the present case. Indeed, the electric potential is $O(\delta^{-1})$

$$\varphi = \delta^{-1}\varphi_{-1} + \varphi_0 + \cdots, \tag{4.2}$$

where

$$\varphi_{-1} \sim -\tilde{E}\bar{r}\cos\theta \quad \text{as} \quad \bar{r} \to \infty. \tag{4.3}$$

We anticipate fluid velocities of the same order [cf. (3.28)],

$$\mathbf{u} = \delta^{-1}\mathbf{u}_{-1} + \mathbf{u}_0 + \cdots. \tag{4.4}$$

A similar expansion applies for the pressure $p$.

We still expect that both $c$ and $q$ are $O(1)$. In fact, Poisson's equation (2.26) gives again

$$q_0 \equiv 0. \tag{4.5}$$

It follows that the salt flux is $O(1)$,

$$\mathbf{j} = \mathbf{j}_0 + \cdots, \tag{4.6}$$

and is dominated by diffusion,

$$\mathbf{j}_0 = -\nabla c_0. \tag{4.7}$$

The current density, on the other hand, is $O(\delta^{-1})$,

$$\mathbf{i} = \delta^{-1}\mathbf{i}_{-1} + \mathbf{i}_0 + \cdots, \tag{4.8}$$

and is dominated by electromigration,

$$\mathbf{i}_{-1} = -c_0 \nabla \varphi_{-1}. \tag{4.9}$$

Substitution into the salt balance (2.24) yields at $O(\delta^{-1})$

$$(m^+ + m^-)\mathbf{u}_{-1}\cdot\nabla c_0 = 0. \tag{4.10}$$

Since $m^{\pm}$ are both positive, salt transport is dominated by advection. With the flow being steady, $c_0$ is constant on each streamline. We make the plausible assumption that the streamlines of $\mathbf{u}_{-1}$ are open, originating at infinity. Since at large distances $c_0 = 1$, we find that

$$c_0 \equiv 1. \tag{4.11}$$

The charge balance (2.25) thus yields at $O(1)$

$$\nabla^2 \varphi_{-1} = 0. \tag{4.12}$$

Poisson's equation (2.26) then implies, again, $O(\delta)$ electroneutrality

$$q_1 \equiv 0. \tag{4.13}$$

The analysis of the outer region is easily continued in this fashion to one higher asymptotic order, yielding

$$c_1 \equiv 0 \tag{4.14}$$

and

$$\nabla^2 \varphi_0 = 0. \tag{4.15}$$

The Coulomb body force in the momentum equation (2.10) thus disappears at $O(\delta^{-1})$:

$$\nabla\cdot\mathbf{u}_{-1} = 0, \quad \nabla p_{-1} = \nabla^2\mathbf{u}_{-1}. \tag{4.16}$$

Before heading to analyze the Debye layer we note that, with an $O(\delta^{-1})$ electric potential, the same scaling holds within the solid,

$$\grave{\varphi} = \delta^{-1}\grave{\varphi}_{-1} + \cdots, \tag{4.17}$$

where $\grave{\varphi}_{-1}$ is harmonic.

### B. Debye scale

We now analyze the inner Debye region. As in the case of moderate fields, we postulate $O(1)$ concentrations

$$c^{\pm} = C_0^{\pm}(Z,\theta) + \cdots. \tag{4.18}$$

Given the $O(\delta^{-1})$ electric field in the outer bulk, we postulate

$$\varphi = \delta^{-1}\Phi_{-1}(\theta) + \Phi_0(Z,\theta) + \cdots, \tag{4.19}$$

where the first term is independent of $Z$; asymptotic matching then implies

$$\Phi_{-1}(\theta) = \varphi_{-1}, \tag{4.20}$$

where, as in the moderate-field analysis, bulk variables appearing in Debye-scale equations are understood to be evaluated at $\bar{r} = 1$. We also postulate an $O(\delta^{-1})$ velocity in the $\theta$ direction,

$$v = \delta^{-1}V_{-1} + \cdots, \tag{4.21}$$

which can match (4.4). The continuity equation and impermeability condition then imply that the radial velocity $u$ is $O(1)$.

As in the moderate-field analysis, the Nernst-Planck equations (2.3) at $O(\delta^{-2})$ in conjunction with the zero ionic flux at $Z = 0$ imply zero transverse ionic fluxes at $O(\delta^{-1})$. We again obtain (3.20), with $\Psi$, as defined by (3.21), being governed by (3.22) and the large-$Z$ decay. In the present case, however, the electric displacement in the solid phase enters Gauss's law (2.13) at $O(\delta^{-1})$; hence the homogeneous equation (3.23) is replaced by

$$\frac{\partial\Psi}{\partial Z}(Z=0,\theta) = \gamma\frac{\partial\grave{\varphi}_{-1}}{\partial r}(r=1,\theta). \tag{4.22}$$

For our purpose, we only need the distribution of $\Psi$ at $Z = 0$ [the $O(1)$ $\zeta$ potential],

$$\zeta(\theta) = \Psi(Z=0,\theta). \tag{4.23}$$

Integration of (3.22) subject to to the requirement of large-$Z$ decay yields

$$\frac{\partial\Psi}{\partial Z} = -2\sinh\frac{\Psi}{2}. \tag{4.24}$$

Substitution of (4.23) and (4.24) into (4.22) yields the equation

$$2\sinh\frac{\zeta}{2} = -\gamma\left.\frac{\partial\grave{\varphi}_{-1}}{\partial r}\right|_{r=1}, \tag{4.25}$$

relating the $\zeta$-potential distribution to the solid polarization.

Lastly, we consider the electrokinetic flow engendered by the intense electric field in the $\theta$ direction. The radial momentum component of (2.10) in conjunction with (4.19) readily implies that the pressure is $O(\delta^{-2})$ and accordingly does not contribute to the $O(\delta^{-3})$ tangential momentum balance

$$\frac{\partial^2 V_{-1}}{\partial Z^2} + \frac{\partial^2\Psi}{\partial Z^2}\frac{d\Phi_{-1}}{d\theta} = 0. \tag{4.26}$$

Integrating twice with respect to $Z$ in conjunction with the no-slip condition and the requirement of asymptotic matching with the $O(\delta^{-1})$ outer flow (which eliminates terms growing as $Z$) yields the velocity profile

$$V_{-1} = (\zeta - \Psi)\frac{d\Phi_{-1}}{d\theta}. \tag{4.27}$$

### C. Effective boundary conditions

Asymptotic matching yields a set of effective boundary conditions governing the outer bulk fields. To begin with, matching the zero $O(\delta^{-1})$ transverse current density in the Debye layer to the ohmic density (4.9) requires that

$$\frac{\partial\varphi_{-1}}{\partial\bar{r}} = 0 \quad \text{at} \quad \bar{r} = 1. \tag{4.28}$$

Next, matching the $O(1)$ radial velocity component within the Debye layer to the $O(\delta^{-1})$ outer flow yields an effective impermeability condition

$$u_{-1} = 0 \quad \text{at} \quad \bar{r} = 1, \tag{4.29}$$

while matching that flow with (4.27) yields a Smoluchowski-type slip condition

$$v_{-1} = \zeta\frac{\partial\varphi_{-1}}{\partial\theta} \quad \text{at} \quad \bar{r} = 1. \tag{4.30}$$

Finally, as the $O(\delta^{-1})$ electric potential does not vary in the $Z$ direction within the Debye layer [see (4.19)], we readily obtain

$$\grave{\varphi}_{-1}|_{r=1} = \varphi_{-1}|_{\bar{r}=1}. \tag{4.31}$$

### D. Induced $\zeta$ potential

The leading-order bulk potential $\varphi_{-1}$ is governed by Laplace's equation (4.12) together with the homogeneous Neumann boundary condition (4.28) and the far-field approach to a uniform field (4.3). The solution to this linear problem is

$$\varphi_{-1} = -\tilde{E}\left(\bar{r} + \frac{1}{2\bar{r}^2}\right)\cos\theta. \tag{4.32}$$

Substituting (4.32) evaluated at $\bar{r} = 1$ into (4.31) yields a boundary condition governing the solid-phase potential $\grave{\varphi}_{-1}$. This harmonic potential is therefore given by

$$\grave{\varphi}_{-1} = -\tfrac{3}{2}\tilde{E}r\cos\theta. \tag{4.33}$$

With the above result, Eq. (4.25) yields the nonlinear $\zeta$-potential distribution

$$\zeta = 2\sinh^{-1}\left(\tfrac{3}{4}\gamma\tilde{E}\cos\theta\right). \tag{4.34}$$

Making use of (4.32), the slip condition (4.30) reads

$$v_{-1} = 3\tilde{E}\sinh^{-1}\left(\tfrac{3}{4}\gamma\tilde{E}\cos\theta\right)\sin\theta. \tag{4.35}$$

This condition uniquely determines the flow.

## V. UNIFORM APPROXIMATION

Consider the leading-order problems governing the outer velocity $\mathbf{u}$ in the moderate- [see (3.37)] and strong-field [see (4.16)] cases. In both limits we found that the flow is governed by the homogeneous Stokes equations

$$\nabla\cdot\mathbf{u} = 0, \quad \nabla p = \nabla^2\mathbf{u}, \tag{5.1}$$

together with impermeability,

$$u = 0 \quad \text{at} \quad \bar{r} = 1, \tag{5.2}$$

and far-field decay. The difference lies in the slip condition: for moderate fields the $O(\delta)$ slip is [see (3.46)]

$$v = \tfrac{9}{4}\delta\gamma E^2 \sin\theta\,\cos\theta, \tag{5.3}$$

corresponding to the $\zeta$-potential distribution $\delta A(\theta)$ [see (3.41) and (3.43)]; at strong fields we have obtained the $O(\delta^{-1})$ slip [see (4.35)]

$$v = 3\delta^{-1}\tilde{E}\,\sinh^{-1}\left(\tfrac{3}{4}\gamma\tilde{E}\,\cos\theta\right)\sin\theta, \tag{5.4}$$

corresponding to the $\zeta$-potential distribution (4.34). Recalling (4.1), we see that (5.4) constitutes a uniform approximation, valid for both moderate and large field values. Using definition (1.1), this approximation simply reads

$$v = 3E\,\sinh^{-1}\left(\tfrac{3}{4}\alpha E\,\cos\theta\right)\sin\theta. \tag{5.5}$$

Similarly, Eq. (4.34) constitutes a uniform approximation for the $\zeta$-potential distribution, namely

$$\zeta = 2\,\sinh^{-1}\left(\tfrac{3}{4}\alpha E\,\cos\theta\right). \tag{5.6}$$

To describe the dependence of the resulting flow upon $E$, it is expedient to identify a global quantity which represents the flow magnitude. We here choose it as the mean slip velocity over one hemisphere (cf. [18,19]),

$$\langle v\rangle = \frac{1}{2\pi}\int_{0<\theta<\pi/2} v\,dA. \tag{5.7}$$

Use of the uniform approximation (5.5) yields

$$\langle v\rangle = 3E\int_0^{\pi/2}\sinh^{-1}\left(\frac{3}{4}\alpha E\,\cos\theta\right)\sin^2\theta\,d\theta. \tag{5.8}$$

Note the invariance to the sign of $E$. For small $\alpha E$, we readily get

$$\langle v\rangle = \tfrac{3}{4}\alpha E^2. \tag{5.9}$$

For large $\alpha E$, use of the approximation

$$\sinh^{-1}x \sim \ln(2|x|)\,\mathrm{sgn}\,x + O(x^{-2}) \quad \text{for} \quad x \gg 1 \tag{5.10}$$

yields

$$\langle v\rangle = \frac{3\pi}{4}|E|\left(\ln\frac{3\alpha|E|}{4} - \frac{1}{2}\right). \tag{5.11}$$

These approximations are illustrated in Fig. 1 for $\alpha = 0.1$, portraying (on a logarithmic scale) a transition from an $E^2$ scaling to an essentially linear growth with $E$.

Another global estimate for the electro-osmotic mechanism is the average of the $\zeta$ potential over one hemisphere,

$$\langle\zeta\rangle = \frac{1}{2\pi}\int_{0<\theta<\pi/2}\zeta\,dA. \tag{5.12}$$

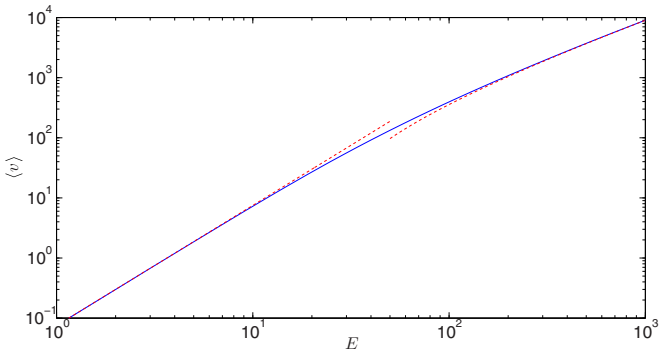


FIG. 1. (Color online) Average velocity $\langle v\rangle$, calculated using (5.8) for $\alpha = 0.1$, as a function of the applied field $E$. Also shown (dashed) are approximations (5.9) and (5.11), respectively corresponding to small and large $\alpha E$.

Use of the uniform approximation (5.6) yields

$$\langle\zeta\rangle = \frac{8}{3\alpha E}\left[\frac{3\alpha E}{4}\sinh^{-1}\frac{3\alpha E}{4} + 1 - \sqrt{1+\left(\frac{3\alpha E}{4}\right)^2}\right]. \tag{5.13}$$

For small $\alpha E$, we readily get

$$\langle\zeta\rangle = \tfrac{3}{4}\alpha E. \tag{5.14}$$

For large $\alpha E$, use of approximation (5.10) yields

$$\langle\zeta\rangle = 2\left(\ln\frac{3\alpha|E|}{2} - 1\right)\mathrm{sgn}(E). \tag{5.15}$$

These approximations are illustrated in Fig. 2, portraying a transition from a linear scaling in $E$ to an essentially logarithmic growth.

It is expedient to supplement the preceding approximations with the limitations imposed upon the value of $E$. Clearly, the entire strong-field analysis breaks down when $\tilde{E}$ becomes comparable to $\delta^{-1}$. Since $\gamma$ is assumed $O(1)$, this means that the strong-field approximation is valid only if

$$E \ll \delta^{-2}. \tag{5.16}$$

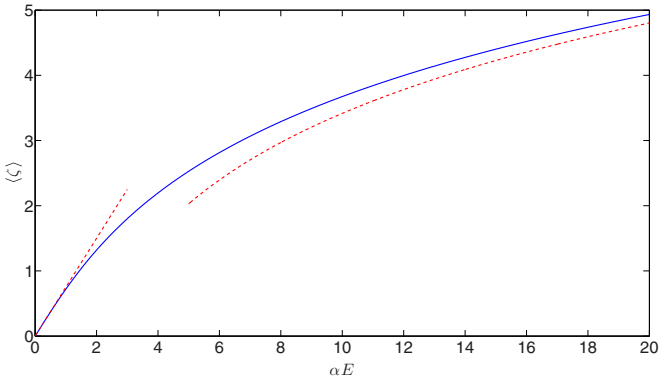


FIG. 2. (Color online) Average $\zeta$ potential $\langle\zeta\rangle$, calculated using (5.13), as a function of $\alpha E$. Also shown (dashed) are approximations (5.14) and (5.15), respectively corresponding to small and large $\alpha E$.

Another restriction,

$$\delta e^{|\zeta|/2} \ll 1, \tag{5.17}$$

follows from the shuffling of terms within the asymptotic hierarchy occurring as the $\zeta$ potentials become moderately large [14]. Application of (5.10) to (4.34) reveals that satisfaction of (5.17) again yields (5.16). Thus, while the induced $\zeta$ potential become logarithmically large for $E \gg \delta^{-1}$, the asymptotic ordering remains intact [20].

## VI. FLOW ABOUT AN INFINITE CIRCULAR CYLINDER

The preceding calculations can easily be carried out for another prototypic configuration, namely an infinite cylinder exposed to a uniform electric field perpendicular to its axis. The two-dimensional transport is naturally described using polar coordinates $(r,\theta)$ with $r = 1$ being the cylinder boundary (corresponding to $a^*$ being the dimensional cylinder radius) and $\theta = 0$ in the applied-field direction. Repeating the analysis, it is readily found that [cf. (5.5)]

$$v = 4E \sinh^{-1}(\alpha E \cos\theta)\sin\theta \tag{6.1}$$

provides a uniform approximation for the electro-osmotic slip. The representative electro-osmotic velocity is here naturally chosen as the average over one quadrant [cf. (5.7)]

$$\langle v\rangle = \frac{2}{\pi}\int_0^{\pi/2} v\, d\theta. \tag{6.2}$$

Use of (6.1) yields here

$$\langle v\rangle = \frac{8}{\pi\alpha}[\alpha E \sinh^{-1}(\alpha E) + 1 - \sqrt{1+\alpha^2E^2}]. \tag{6.3}$$

The analogs of (5.9) and (5.11) are

$$\langle v\rangle = \frac{4}{\pi}\alpha E^2 \quad \text{for} \quad \alpha E \ll 1 \tag{6.4}$$

and

$$\langle v\rangle = \frac{8|E|}{\pi}[\ln(2\alpha|E|) - 1] \quad \text{for} \quad \alpha E \gg 1. \tag{6.5}$$

## VII. CONCLUDING REMARKS

We have analyzed the electro-osmotic flow engendered about a dielectric particle of zero surface charge. Our key result is the uniform approximation (5.5) for the electro-osmotic slip. Assuming typical solids encountered in electrokinetic applications, where $\gamma$ is at most moderate, the polarization parameter $\alpha$ is $O(\delta)$. Approximations (5.9) and (5.11) for the average slip accordingly describe a transition from the velocity scaling $\delta E^2$ at moderate fields [$E \lesssim O(1)$] to the newly identified scaling $|E|\ln(\delta|E|)$ at intense fields [$\delta^{-1} \ll E \ll \delta^{-2}$].

Practically speaking, logarithmic terms may be considered $O(1)$, in agreement with the numerical values they realistically attain. At intense fields, the dimensionless fluid velocity thus scales essentially as $|E|$. In a dimensional notation [see (2.2)], we have revealed here a transition from a velocity scale that is proportional to the Debye width [see (2.7)] to one that is independent of it; both scales are independent of particle size.

It is of interest to compare the present velocity scalings to those pertaining to induced-charge flows about a perfectly conducting (i.e., metal) sphere of zero net charge. In that problem, the induced $\zeta$ potential scales as $E$ at moderate fields [2]; the dimensionless velocity thus scales as $E^2$, representing dimensional velocities that are linear in particle size. These velocities, of course, are much larger than those predicted in the present problem under moderate fields. It is well understood, however, that the rapid growth with $E$ of the induced $\zeta$ potential about a perfect conductor introduces both nondilute [21,22] and surface-conduction [14] effects already at moderately large values of $E$; additionally, recent numerical simulations of the exact Poisson-Nernst-Planck equations about a cylinder predict an inherent instability occurring beyond $E \approx 30$ [23]. The large velocities predicted by the weak-field theories are simply not realized, and the velocity scaling at large values of $E$ is yet unknown [24].

No such complications arise in the present problem of an uncharged dielectric surface, where the $\zeta$ potential, albeit induced, grows only mildly with the applied field, and surface conduction is negligible even for $E \gg \delta^{-1}$. We therefore conjecture that at sufficiently strong fields the induced electro-osmotic velocities may be *larger* than those attained in the flow about a perfect conductor. This suggests the need for a revision in our perception of induced-charge electro-osmosis. Following the introduction of this concept into the western literature [1,2], the common view was that the induced-charge mechanism can lead, through a field-square scaling, to large velocities which are not attained in standard electro-osmotic flows about a charged dielectric solid. It has since been found that these predictions are both qualitatively and quantitatively incompatible with experimental observations [25]. We propose that large velocities might actually be achieved in the related phenomena of induced-charge flows about uncharged dielectric surfaces, traditionally assumed asymptotically small.

## ACKNOWLEDGMENTS

This work was supported by the Israel Science Foundation (Grant No. 184/12).

[1] M. Z. Bazant and T. M. Squires, Phys. Rev. Lett. **92**, 066101 (2004).
[2] T. M. Squires and M. Z. Bazant, J. Fluid Mech. **509**, 217 (2004).
[3] One may claim that, in the microscopic level, the solid polarization does represent such surface charges. This is however irrelevant to the present discussion, since electrokinetic phenomena are naturally described on the macroscopic level.
[4] Mathematically, the formation of a diffuse-charge layer represents the nonuniformity of the limit of thin Debye layers, where a small parameter multiplies the highest derivative in Poisson's equation. It is customary to associate the formation of that layer with the presence of charge on the solid surface; the case of an uncharged dielectric reveals that this is not necessary.
[5] F. Zhang and D. Li, J. Colloid Interface Sci. **410**, 102 (2013).

[6] We suspect that this is partly due to the seminal paper of O'Brien and White [26], where it was found that the specific form of the electrostatic boundary condition at the solid-liquid interface does not affect the electrophoretic velocity at weak fields.
[7] S. K. Thamida and H.-C. Chang, Phys. Fluids **14**, 4315 (2002).
[8] G. Yossifon, I. Frankel, and T. Miloh, Phys. Fluids **18**, 117108 (2006).
[9] P. Takhistov, K. Duginova, and H.-C. Chang, J. Colloid Interface Sci. **263**, 133 (2003).
[10] F. Nadal, F. Argoul, P. Kestener, B. Pouligny, C. Ybert, and A. Ajdari, Eur. Phys. J. E **9**, 387 (2002).
[11] G. Yossifon, I. Frankel, and T. Miloh, Phys. Fluids **19**, 068105 (2007).
[12] E. Yariv and A. M. J. Davis, Phys. Fluids **22**, 052006 (2010).
[13] In fact, $\gamma$ can be quite small when considering aqueous solutions: for polystyrene, for example, it is about $1/40$.
[14] O. Schnitzer and E. Yariv, Phys. Rev. E **86**, 021503 (2012).
[15] J. Kim and D. F. Lawler, Bull. Korean Chem. Soc. **26**, 1083 (2005).
[16] D. A. Saville, Annu. Rev. Fluid Mech. **9**, 321 (1977).
[17] E. Yariv, Chem. Eng. Commun. **197**, 3 (2009).
[18] E. Yariv and T. Miloh, J. Fluid Mech. **595**, 163 (2008).
[19] M. M. Gregersen, M. B. Andersen, G. Soni, C. Meinhart, and H. Bruus, Phys. Rev. E **79**, 066316 (2009).
[20] With the present velocity scaling, it may appear that surface conduction should affect the leading-order transport even when (5.17) is satisfied. Following the analysis of a related problem [27] it may be verified, however, that the $O(1)$ salt flux emanating out of the Debye layer are accommodated in a diffusive boundary layer where the deviation of the salt concentration from the uniform reference value is asymptotically small. The preceding analysis therefore remains intact.
[21] M. Z. Bazant, M. S. Kilic, B. D. Storey, and A. Ajdari, New J. Phys. **11**, 075016 (2009).
[22] M. Z. Bazant and T. M. Squires, Curr. Opin. Colloid Interface Sci. **15**, 203 (2010).
[23] S. Davidson, M. B. Andersen, and A. Mani, Phys. Rev. Lett. **112**, 128302 (2014).
[24] It is also illuminating to compare the present results to those describing electrophoresis of a *charged* dielectric sphere. Here, the electrophoretic particle velocity naturally provides a lumped characteristic estimate of the typical electro-osmotic velocity in the problem. (In fact, this velocity is provided by the mean value of the electro-osmotic slip.) Considering (the practically common case of) moderate surface charges, where the $\zeta$ potentials are comparable with the thermal voltage, surface conduction does not affect the leading-order transport [14]. Thus Smoluchowski's formula applies for moderate fields, essentially providing $E$ as the typical velocity scale. As explained in Ref. [28], however, this formula breaks down for $E \sim O(\delta^{-1})$; at intense fields, $\delta^{-1} \ll E \ll \delta^{-2}$, the dependence upon $E$ becomes weak (i.e., logarithmic), and the electrophoretic velocity essentially scales as $\delta^{-1}$—see Eq. (5.13) in Ref. [28]. (The weak dependence upon $E$ results from a subtle cancellation of slip contribution.) In a dimensional notation, this represents a transition from a velocity scale that is size independent to one that scales inversely with the Debye width.
[25] M. Z. Bazant, M. S. Kilic, B. D. Storey, and A. Ajdari, Adv. Colloid Interface Sci. **152**, 48 (2009).
[26] R. W. O'Brien and L. R. White, J. Chem. Soc., Faraday Trans. **74**, 1607 (1978).
[27] O. Schnitzer and E. Yariv, J. Fluid Mech. **701**, 333 (2012).
[28] O. Schnitzer and E. Yariv, Phys. Fluids **24**, 082005 (2012).